PLANT BIOLOGY

Plasmodesmata-localized proteins and ROS orchestrate light-induced rapid systemic signaling in *Arabidopsis*

Yosef Fichman[1], Ronald J. Myers Jr.[1], DeAna G. Grant[2], Ron Mittler[1,3]*

Copyright © 2021 The Authors, some rights reserved; exclusive licensee American Association for the Advancement of Science. No claim to original U.S. Government Works

Systemic signaling and systemic acquired acclimation (SAA) are key to the survival of plants during episodes of abiotic stress. These processes depend on a continuous chain of cell-to-cell signaling events that extends from the initial tissue that senses the stress (the local tissue) to the entire plant (systemic tissues). Reactive oxygen species (ROS) and Ca^{2+} are key signaling molecules thought to be involved in this cell-to-cell mechanism. Here, we report that the systemic response of *Arabidopsis thaliana* to a local treatment of high light stress, which resulted in local ROS accumulation, required ROS generated by respiratory burst oxidase homolog D (RBOHD). ROS increased cell-to-cell transport and plasmodesmata (PD) pore size in a manner dependent on PD-localized protein 1 (PDLP1) and PDLP5, and this process was required for the propagation of the systemic ROS signals and SAA. Furthermore, aquaporins and several Ca^{2+}-permeable channels in the glutamate receptor–like (GLR), mechanosensitive small conductance–like (MSL), and cyclic nucleotide–gated (CNGC) families were involved in this systemic signaling process. However, we determined that these channels were required primarily to amplify the systemic signal in each cell along the path of the systemic ROS wave, as well as to establish local and systemic acclimation. Thus, PD and RBOHD-generated ROS orchestrate light stress–induced rapid cell-to-cell spread of systemic signals in *Arabidopsis*.

INTRODUCTION

Acclimation of plants to changes in their environment requires many different physiological, molecular, and metabolic responses. These are controlled by multiple signal transduction cascades, hormonal signaling pathways, and changes in steady-state concentrations of Ca^{2+} and reactive oxygen species (ROS) (*1*–*4*). In addition to activating acclimation mechanisms at the specific tissue(s) exposed to stress, different abiotic stresses, as well as mechanical injury, can trigger rapid systemic signaling pathways that result in systemic acquired acclimation (SAA) or systemic wound responses (SWRs) throughout the whole plant (*5*–*18*). In the case of abiotic stresses, such as high light (HL) or heat stresses, rapid systemic signaling and SAA protect the plant from a subsequent exposure to the same stress (*9*, *14*, *19*–*22*).

Among the many different systemic signaling pathways thought to mediate rapid systemic responses and SAA or SWR are electrical, Ca^{2+}, hydraulic, and ROS waves (*6*–*8*, *10*, *12*, *13*, *21*–*23*). Electrical signals and Ca^{2+} waves occurring during SWR depend on the Ca^{2+}-permeable glutamate receptor–like (GLR) channels GLR3.3 and GLR3.6 (*7*, *10*, *13*, *23*), and Ca^{2+} and ROS waves occurring during systemic responses to HL or salt stress are thought to be linked through the function of the respiratory burst oxidase homolog D (RBOHD) protein (*6*, *15*, *17*, *24*, *25*). RBOHD is also required for the propagation of electric signals in response to HL stress (*14*). Although it is not known how hydraulic waves are linked to electric, Ca^{2+}, and ROS waves, it has been proposed that members of the mechanosensitive channels of small conductance–like [MSL; (*26*)] family, which are permeable to Ca^{2+} and/or other cations and anions, could sense systemic hydraulic waves at tissues distant from the site of stress and convert them into Ca^{2+} signals (*4*, *17*, *24*). Ca^{2+} signals can further affect ROS signals through the function of many different Ca^{2+}-binding proteins and/or Ca^{2+}-dependent kinase and/or phosphatase switches or by directly binding to the EF-binding domains of the RBOHD protein (*1*–*4*, *24*, *25*). Other Ca^{2+}-permeable channels proposed to be involved in regulating local and/or systemic responses to stress include cyclic nucleotide–gated ion channels [CNGCs; (*27*)], annexins [ANNs; (*28*)], reduced hyperosmolality-induced [Ca^{2+}]i increase [OSCA; (*29*)], and two-pore channel [TPC; (*30*)].

The activation of RBOHD at the plasma membrane (PM) results in the generation of superoxide (O_2^-) molecules that dismutate into hydrogen peroxide (H_2O_2) in the apoplast, the compartment between the plant PM and cell wall. Aquaporins such as PM-intrinsic protein channels [PIPs; (*31*, *32*)] transport H_2O_2 across the PM from the apoplast into the cytosol. The translocation of H_2O_2 into the cytosol enables it to alter different redox-dependent reactions, kinase and/or phosphatase molecular switches, and/or Ca^{2+}-permeable channels, further driving different local and systemic acclimation pathways (*6*, *8*, *9*, *19*–*22*, *25*, *31*). This type of apoplast-to-cytosol translocation of signaling molecules such as H_2O_2 is also responsible for cell-to-cell communication of systemic signals during SAA (*6*, *8*, *9*, *18*–*22*). Because the apoplastic space is continuous between neighboring plant cells, a signaling compound, such as H_2O_2, produced by one cell could enter a neighboring cell and trigger acclimation and defense mechanisms in it, resulting in the activation of its own RBOHD, and a chain of cell-to-cell transmission of this type of signal (the ROS wave) could mediate rapid systemic signaling (*6*, *8*, *14*, *19*–*22*, *33*–*35*). In addition to such an apoplastic route of H_2O_2-to-cytosol translocation among different cells during systemic signaling, a symplastic route of systemic signaling through plasmodesmata (PD), structures that connect the cytoplasm of adjacent cells, could play a role in the translocation of systemic signals, mediating different Ca^{2+}, redox, or kinase and/or phosphatase switch modes between cells (*7*, *17*, *36*–*38*). Proteins such as PD-localized

[1]The Division of Plant Sciences and Interdisciplinary Plant Group, College of Agriculture, Food and Natural Resources, Christopher S. Bond Life Sciences Center, University of Missouri, 1201 Rollins St, Columbia, MO 65201, USA. [2]Electron Microscopy Core Facility, University of Missouri, W136 Veterinary Medicine Building 1600 East Rollins Street, Columbia, MO 65211, USA. [3]Department of Surgery, University of Missouri School of Medicine, Christopher S. Bond Life Sciences Center, University of Missouri, 1201 Rollins St, Columbia, MO 65201, USA.
*Corresponding author. Email: mittlerr@missouri.edu

Downloaded from http://stke.sciencemag.org/ on June 24, 2021

proteins 1 and 5 [PDLP1 and PDLP5; (*39*)], PM-localized leucine-rich repeat receptor-like kinase 7 [KIN7; (*40*)], and green fluorescent protein (GFP)–arrested trafficking 1 [GAT1; (*41*)] affect translocation through PDs. However, roles for these proteins in stimulating or repressing systemic responses at the rapid rate required for SAA to be effective (*4*) have not been demonstrated. In addition, although PD pore size has been proposed to be controlled by changes in redox levels (*42*–*45*), whether or not PD transport is affected by ROS during rapid systemic signaling and SAA to HL stress is currently unknown.

To address the challenge of imaging ROS in live plants growing in soil, we developed a method that delivers different ROS-sensitive dyes into plants through fumigation (*8*, *20*–*22*, *46*). After the application of the dyes, the accumulation of ROS can be visualized in whole plants in response to different local stimuli using an imager similar to that used to image whole mice, such as an IVIS Lumina 5 platform (*8*, *20*–*22*, *46*). Here, using this method, coupled with grafting and acclimation assays, we studied how systemic signaling is altered in wild type and many different *Arabidopsis thaliana* mutants impaired in ROS, Ca^{2+}, PD, and aquaporin functions (table S1), in response to a local application of HL stress. We found that the propagation of systemic ROS signals in response to a local treatment of HL stress required the function of the ROS-generating enzyme RBOHD and two other proteins involved in regulating different PD functions (PDLP1 and PDLP5). In contrast, aquaporins and several Ca^{2+}-permeable channels (GLRs, MSLs, and CNGC2) were primarily required for amplification of the systemic ROS signal in each cell along the path of the systemic signal, as well as for the establishment of local and systemic acclimation. ROS produced by RBOHD was further found to be required for opening of PD pores during rapid systemic signaling.

RESULTS

Ca^{2+}-permeable channels regulate generation and propagation of rapid systemic ROS signals in *Arabidopsis*

Ca^{2+} and ROS signaling are thought to co-regulate many of the different responses of plants to changes in environmental conditions (*1*, *2*, *4*). The double-mutant *glr3.3;glr3.6* is blocked in the propagation of systemic electric signals and Ca^{2+} waves in response to wounding (*7*, *10*, *13*, *23*), highlighting the importance of GLR3.3 and GLR3.6 for systemic signaling. In our hands, however, rapid systemic ROS signaling in response to a local HL stress treatment [not injury, as in (*7*, *10*, *13*, *23*)], in the *glr3.3;glr3.6* double mutant, was not blocked, but rather reduced (Fig. 1A and movie S1). Moreover, the single *glr3.3* mutant displayed an enhanced rate of systemic ROS signal propagation, whereas the single *glr3.6* mutant was similar to wild type in response to the local application of HL (fig. S1 and table S1). Other Ca^{2+}-permeable channels that could alter cytosolic Ca^{2+} concentrations and activate ROS production by RBOHD are CNGCs (*27*) and MSLs (*26*). In contrast to the double *glr3.3;glr3.6* mutant, two independent alleles, each of *cngc2* (Fig. 1B and movie S2) and *msl2* (Fig. 1C and movie S3), were completely deficient in the induction and/or propagation of the rapid systemic ROS signal in response to a local HL treatment. Although similar results were found with two independent alleles each of *msl3* (fig. S2), two independent alleles, each of a large number of other mutants for Ca^{2+}-permeable channels, including *msl10*, *ann1*, *osca1*, and *tpc1*, displayed an enhanced rate of systemic ROS signal propagation in response to a local application of HL stress (figs. S3 to S6 and table S1).

These results suggest that many different Ca^{2+}-permeable channels are involved in regulating the formation and/or propagation of systemic ROS signals in plants. Some, such as *glr3.3;glr3.6*, *msl2*, *msl3*, and *cngc2*, are required, whereas others, for example, *ann1*, *tpc1*, *msl10*, and *osca1*, could play a repressive or inhibitory role. The differences observed between the single (fig. S1) and double (Fig. 1A) *glr3.3* and *glr3.6* mutants could reflect the interactions between ROS and Ca^{2+} signaling in the different cell layers of the vascular system of plants. Whereas GLR3.3 is localized to the phloem and GLR3.6 to the xylem parenchyma, RBOHD is present in both layers (*10*, *13*, *22*, *24*). The differential function of the two different GLRs in the two different cell layers, coupled with their possible interactions with RBOHD, could therefore result in the differences observed in our study between ROS signaling in the single and double GLR mutants (Fig. 1A and fig. S1). The finding that at least three different types of Ca^{2+}-permeable channels (GLR, CNGC, and MSL; Fig. 1, A to C) are required for mediating rapid systemic ROS signaling in *Arabidopsis* underscores the tight level of regulation and coordination required for this process to occur.

PD and aquaporins play key roles in regulating rapid systemic ROS signals in *Arabidopsis*

Although much is known about Ca^{2+} and ROS integration during responses to changes in abiotic and biotic conditions (*1*–*4*, *6*, *7*, *10*, *13*, *15*, *24*), less is known about the role of PD and aquaporins in these responses. To determine whether local HL stress–induced systemic signaling in *Arabidopsis* uses an aquaporin-associated apoplastic route or a PD-dependent symplastic route for ROS wave initiation and/or propagation, we measured local HL stress–induced systemic ROS signals in different mutants impaired in aquaporin or PD functions. Mutants for *pdlp1* or *pdlp5* (two independent alleles of each) were impaired in mediating the rapid systemic ROS signal in response to a local application of HL stress (Fig. 2, A and B; movies S4 and S5; and table S1). In contrast, two other PD mutants, *kin7* and *gat1* (two independent alleles of each), displayed enhanced or wild-type–like rates of systemic ROS signal propagation, respectively (figs. S7 and S8 and table S1). Two independent alleles of the aquaporin mutant *pip1;2* had an enhanced rate of systemic ROS signal propagation (Fig. 2C, movie S6, and table S1), whereas two independent alleles of the aquaporin *pip2;1* were completely deficient in the initiation and propagation of the rapid systemic ROS signal (Fig. 2D, movie S7, and table S1). In contrast, *pip1;4* (two independent alleles) displayed a wild-type–like systemic ROS response (fig. S9 and table S1).

The finding that PIP2;1, which localizes to vascular bundles in *Arabidopsis* (*31*, *32*), is essential for the initiation and/or propagation of the ROS wave (Fig. 2D, movie S7, and table 1) is in agreement with our findings that rapid systemic ROS signaling occurs through phloem and xylem parenchyma cells during systemic responses to HL stress (*22*). Similar to Ca^{2+}-permeable channels (Fig. 1, A to C), the function of different aquaporins, which could mediate ROS movement between the apoplast and the cytosol (*31*, *32*), and PD-related proteins, which could regulate the movement of redox state, Ca^{2+}, and/or other signals between cells (*37*–*45*), might be required within the same cell or in different cells for mediating rapid systemic signals in plants. Our findings indicate therefore that both

Downloaded from http://stke.sciencemag.org/ on June 24, 2021

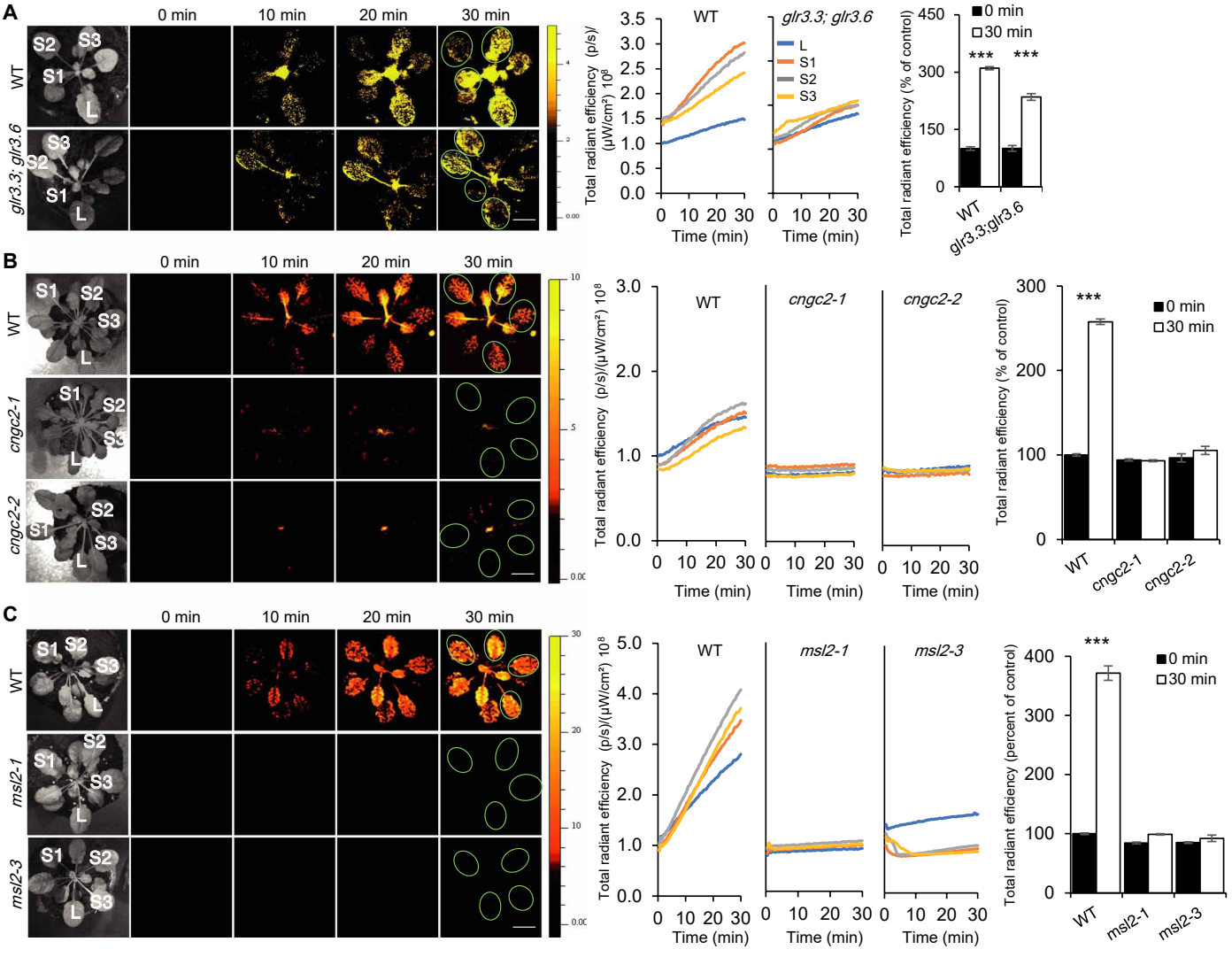

Fig. 1. Multiple types of Ca^{2+}-permeable channels are required for light stress–induced rapid systemic ROS signaling in *Arabidopsis*. (**A**) *Arabidopsis* plants were subjected to a local high light (HL) stress treatment applied to leaf L only. Local (L) and systemic (S) ROS were measured in leaves L and S1 to S3, respectively. Representative time-lapse images of local and systemic ROS accumulation in wild-type (WT) and *glr3.3;glr3.6* double mutants are shown alongside representative line graphs showing continuous measurements of local and systemic ROS in each leaf over the entire course of the experiment. Regions of interest (local and systemic leaves) are indicated by ovals in the images. The bar graph shows combined data from all plants used for the analysis at the 0- and 30-min time points. (**B**) Same as in (A) but for WT and two independent alleles of *cngc2*. (**C**) Same as in (A) but for WT and two independent alleles of *msl2*. All experiments were repeated at least three times with 10 plants of each genotype per experiment. Student's *t* test, SE, $N = 30$ per genotype, $^{***}P < 0.005$. Scale bar, 1 cm.

symplastic and apoplastic routes of intercellular exchange could be required for rapid systemic signaling in *Arabidopsis*.

Mutants deficient in Ca^{2+}-permeable channels, PD, and aquaporin functions are also deficient in local HL stress–induced SAA

The triggering of SAA by systemic signals is thought to play a key role in plant survival during episodes of abiotic stress (*1*–*4*, *9*, *14*, *19*–*22*). To determine whether the block or suppression in rapid systemic signaling displayed in the different mutants described above (Figs. 1, A to C, and 2, B and D) affected acclimation to HL stress (*9*, *14*, *19*–*22*), we tested the systemic and local acclimation of *glr3.3;glr3.6*, *cngc2*, *msl2*, *pip2;1*, and *pdlp5* mutants to an extended HL stress treatment after a short local treatment of HL stress. All mutants tested were impaired, albeit to various degrees, in systemic or local acclimation to HL stress (Fig. 3A). To further study acclimation in local and systemic tissues of these mutants, we measured the abundance of acclimation-associated transcripts *ZAT10*, *ZAT12*, and *MYB30* [previously found to respond to HL stress at the local and systemic leaves of wild-type plants; (*6*, *9*, *20*, *21*)]. Expression of *ZAT10* and *ZAT12* was enhanced in the local leaves that were directly subjected to the HL treatment in all mutants (Fig. 3B). With the exception of *glr3.3;glr3.6*, which displayed suppressed expression of acclimation transcripts in systemic leaves, the expression of *ZAT10* and *ZAT12* in systemic tissues of all other mutants was blocked (Fig. 3B). In addition, and in agreement with the lack of systemic tissue acclimation to HL stress (Fig. 3A), the expression of *MYB30*, which is required for systemic, but not local, acclimation to HL stress (*21*), was

Downloaded from http://stke.sciencemag.org/ on June 24, 2021

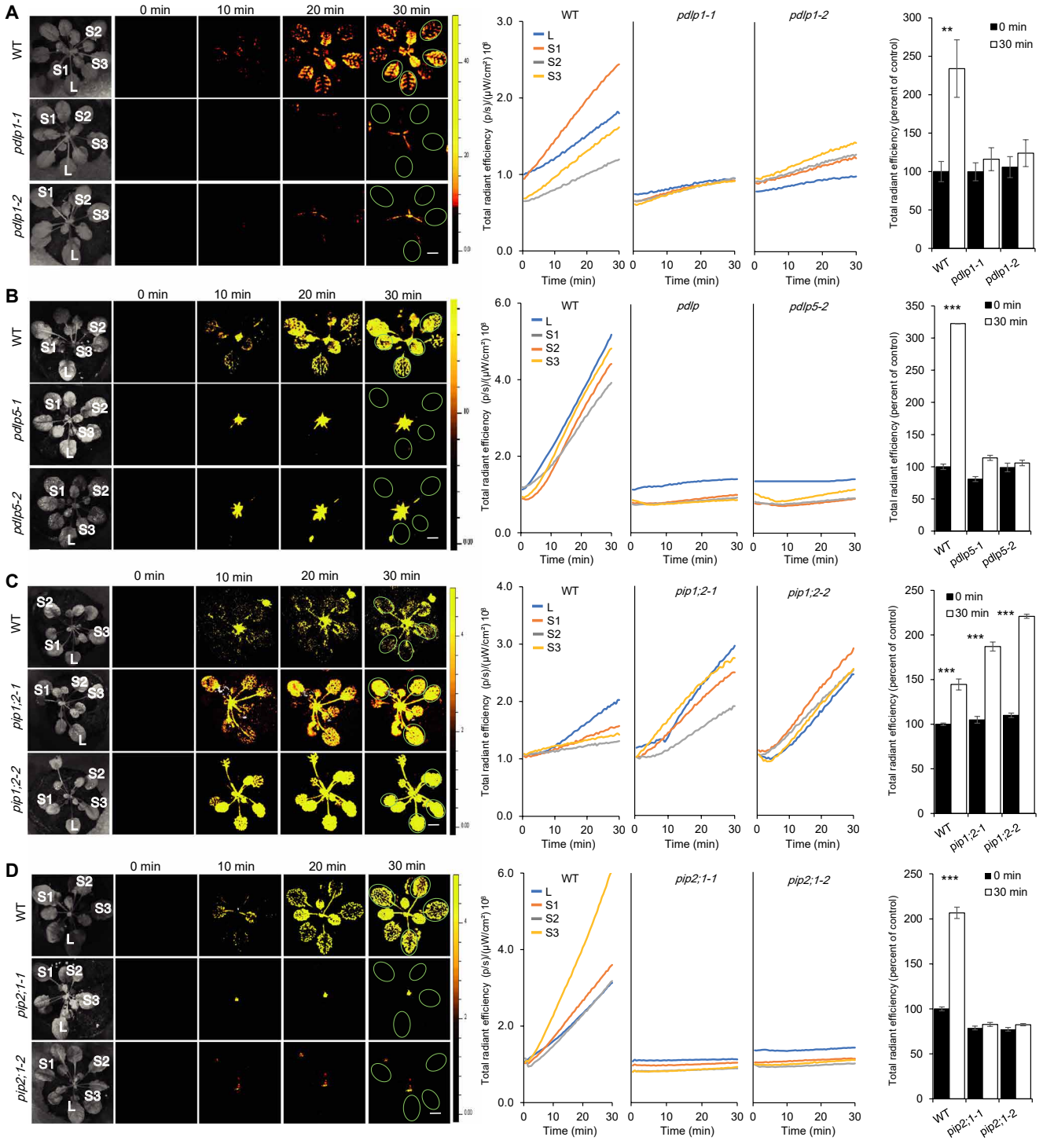

Fig. 2. PDLP1, PDLP5, and PIP2;1 are required for light stress–induced rapid systemic ROS signaling in *Arabidopsis*. (**A**) *Arabidopsis* plants were subjected to a local HL stress treatment applied to leaf L only. Local (L) and systemic (S) ROS were measured in leaves L and S1 to S3, respectively. Representative time-lapse images of systemic ROS accumulation in WT and *pdlp1* (two independent alleles) are shown alongside representative line graphs showing continuous measurements of local and systemic ROS levels in each leaf over the entire course of the experiment. Regions of interest (local and systemic leaves) are indicated by ovals in the images. The bar graph shows combined data of all plants used for the analysis at the 0- and 30-min time points. (**B**) Same as in (A) but for WT and two independent alleles of *pdlp5*. (**C**) Same as in (A) but for WT and two independent alleles of *pip1;2*. (**D**) Same as in (A) but for WT and two independent alleles of *pip2;1*. All experiments were repeated at least three times with 10 plants of each genotype per experiment. Student's *t* test, means ± SE, $N = 30$ per genotype, $^{***}P < 0.005$ and $^{**}P < 0.01$. Scale bar, 1 cm.

Downloaded from http://stke.sciencemag.org/ on June 24, 2021

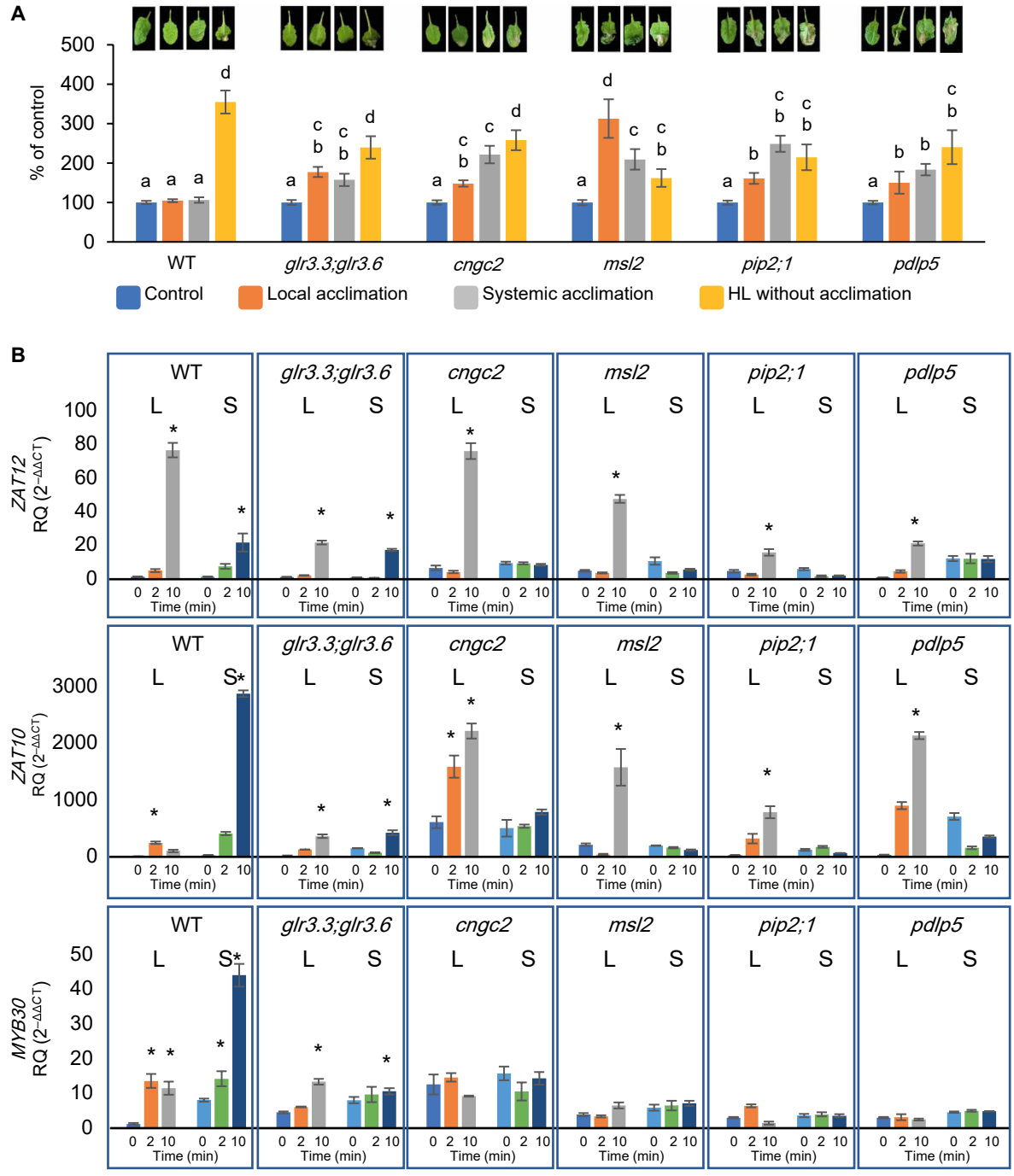

Fig. 3. Acclimation of mutants impaired in light stress–induced systemic ROS signaling. (**A**) Representative leaf images and averaged measurements of leaf injury (increase in ion leakage) for wild-type and *glr3.3;glr3.6*, *cngc2*, *msl2*, *pip2;1*, and *pdlp5* mutants. Measurements are shown for unstressed plants (control), local leaves subjected to a pretreatment of HL stress before a long HL stress period (local acclimation), systemic leaves of plants subjected to local HL stress pretreatment before a long period of HL stress was applied to the systemic leaf (systemic acclimation), and systemic leaves of plants subjected to a long HL stress period without pretreatment (HL without acclimation). Results are presented as percentage of control (leaves not exposed to any HL stress). (**B**) Real-time qPCR analysis of *ZAT12*, *ZAT10*, and *MYB30* expression in local and systemic leaves of wild-type and the *glr3.3;glr3.6*, *cngc2*, *msl2*, *pip2;1*, and *pdlp5* mutants subjected to a local HL treatment. Results are presented as relative quantity (RQ; $2^{-\Delta\Delta CT}$) compared to internal control [elongation factor 1α (EF-1α)] and time 0. All experiments were repeated at least three times with at least 10 plants of each genotype per experiment. Data represent means ± SE, $^*P < 0.05$. Acclimation experiments were analyzed using a one-way ANOVA followed by a Tukey's post hoc test, and transcript expression analysis was analyzed using a Student's *t* test.

Downloaded from http://stke.sciencemag.org/ on June 24, 2021

repressed in the systemic tissues of all mutants (Fig. 3B). These results demonstrate that the different mutants tested were able to sense the stress at the local tissues that were exposed to the stress but were unable to transmit the systemic signal from the local stressed tissues to the systemic leaves or, in the case of *glr3.3;glr3.6*, had a reduced rate of systemic signal transmission. The disruption or suppression in systemic signaling, caused by mutations in the *GLR3.3;GLR3.6*, *CNGC2*, *MSL2*, *PIP2;1*, or *PDLP5* genes (Figs. 1, A to C, and 2, B and D, and table S1), was therefore detrimental for plant acclimation to stress (Fig. 3A), underscoring the important biological roles these proteins play in this process.

Grafting experiments reveal differential roles for Ca^{2+}-permeable channels, PD, and aquaporin in systemic ROS signaling after local HL stress

Because the suppressed ability of mutants impaired in *GLR3.3; GLR3.6*, *CNGC2*, *MSL2*, *PIP2;1*, or *PDLP5* function to systemically acclimate to HL stress (Fig. 3A) could result from their inability to initiate and/or propagate the rapid systemic signal, we conducted grafting experiments (*47*) between wild-type plants and the *glr3.3; glr3.6*, *cngc2*, *msl2*, *pip2;1*, *pdlp5*, and *pdlp1* mutants (Fig. 4A). As controls, we conducted grafting experiments between wild-type plants and between wild-type plants and *rbohD* mutants, which have reduced systemic apoplastic ROS accumulation in response to local HL stress treatment (*6*, *8*), are unable to induce SAA in response to a local application of HL stress (*9*, *18*), and are unable to transmit a heat stress–induced systemic signal generated in a wild-type stock to the mutant scion (*14*). In our grafting experiments, a donor branch from one plant (the scion) was grafted onto a recipient plant grown in soil (the stock). The scion graft was from either a wild-type plant or a mutant, and the stock plant was either a wild-type plant or a mutant; all possible combinations were performed for wild type and the different *glr3.3;glr3.6*, *cngc2*, *msl2*, *pip2;1*, *pdlp5*, and *pdlp1* mutants. Only grafts that remained green and maintained turgor for up to 10 or more days after the grafting procedure, an indication of successful grafting (*47*), were used for analysis, and multiple successful grafting events were obtained for all mutants described above. In all experiments, the HL stress treatment was applied to one leaf belonging to the stock (the local leaf), and the entire plant (stock with the scion graft attached to it) was imaged to detect ROS accumulation at the local and systemic tissues.

Grafting experiments between *rbohD* and wild type demonstrated that the *rbohD* mutant was unable to mediate systemic ROS signaling whether the mutant tissue was the scion or the stock, showing that RBOHD was absolutely required for both initiating and propagating the systemic ROS signal in response to HL stress (Fig. 4, B and C, and fig. S10A). The systemic ROS signal did not therefore initiate in the *rbohD* stock, nor did it propagate through the *rbohD* scion, after a local HL stress treatment of the *rbohD* or wild-type stocks, respectively. The only other mutants that displayed a similar behavior were *pdlp1* and *pdlp5*, indicating that PD function is also absolutely required along the entire path of the systemic signal (Fig. 4, B and C, and fig. S10, E and F). In contrast, the grafting results in which the *glr3.3;glr3.6*, *cngc2*, *msl2*, and *pip2;1* mutants were used as scion or stock suggested that the protein products of these genes may have cell-autonomous functions (Fig. 4, A to C, and fig. S10, B to D). They may not be required for the initiation or the propagation of the systemic ROS signal, because the systemic signal could be initiated and propagated through a stock of these mutants, which do not show enhanced ROS accumulation, and proceed through this stock into a wild-type scion in which it caused systemic ROS accumulation (Fig. 4, A to C, and fig. S10, B to D). In contrast, however, once the systemic ROS signal was initiated in a wild-type stock, it did not further propagate through a scion derived from these mutants, and these scion sections did not display enhanced systemic ROS accumulation (Fig. 4, A to C, and fig. S10, B to D). *RBOHD*, *PDLP5*, and *PDLP1* were therefore required for the initiation and propagation of the rapid systemic ROS signal between cells, whereas *GLR3.3;GLR3.6*, *CNGC2*, *MSL2*, and *PIP2;1* were required for the amplification and/or maintenance of the systemic ROS signal in each individual cell (Fig. 4, A to C, and fig. S10, A to G).

RBOHD and *PDLP5* enable cell-to-cell spread of carboxyfluorescein and increase PD pore size during responses to local HL stress

The findings that *RBOHD*, *PDLP1*, and *PDLP5* were required for the propagation of the rapid systemic ROS signal from local to systemic tissues (Fig. 4, A to C, and fig. S10, A to G) could suggest that ROS and PD functions are interlinked during systemic signaling. Increased ROS concentrations are proposed to enhance transport through PD and tunneling nanotubes in plant and mammalian cells, respectively (*45*). If such a mechanism occurs in *Arabidopsis* in response to a local HL stress treatment, it could explain why RBOHD and PDLPs are both required for systemic ROS signaling in *Arabidopsis* (Figs. 2, A and B, 3, A and B, and 4, B and C). To test this possibility, we measured the cell-to-cell spread of the fluorescent compound carboxyfluorescein (*48*) in local and systemic leaves of wild-type, *rbohD*, and *pdlp5* plants that were untreated or treated with a 2-min HL stress. The spread of carboxyfluorescein was measured in vascular tissues and the parenchyma by using two different methods for loading the leaves with the fluorescent compound (fig. S11A). Although carboxyfluorescein spread was facilitated in response to a local HL stress treatment in petioles and leaf cells of local and systemic leaves of wild-type plants, a similar response was not observed in the petioles and leaf cells of local or systemic leaves of *rbohD* and *pdlp5* plants (Fig. 5, A and B).

Because ROS are proposed to increase PD pore size, facilitating PD transport by a factor of ~10 (*45*), we used transmission electron microscopy [TEM; (*49*)] to measure PD pore size in petioles of local leaves from wild-type, *rbohD*, and *pdlp5* plants treated or untreated for 2 min with local HL stress, focusing on vascular bundle and parenchyma cells (fig. S11B). The pore area of PD (categorized as either H/M- or X/Y-shaped PDs) from wild-type plants increased in response to local HL stress treatment (Fig. 5, A and B), in agreement with the facilitated spread of carboxyfluorescein after local HL stress treatment. In contrast, the PD pore area in *rbohD* and *pdlp5* plants decreased (Fig. 5C), in agreement with the lack of local HL stress–driven facilitated carboxyfluorescein spread in these mutants (Fig. 5, A and B). These findings suggest that RBOHD-generated ROS promote cell-to-cell transport and PD pore area size in a PDLP5-dependent manner.

DISCUSSION

The findings presented here suggest that PD regulation (PDLP5 and PDLP1) and ROS production (RBOHD) are required along the entire path of the HL stress–induced rapid systemic ROS signal (Figs. 2, A and B, 3, A and B, 4, B and C, and 5, A and B). In contrast, the

Downloaded from http://stke.sciencemag.org/ on June 24, 2021

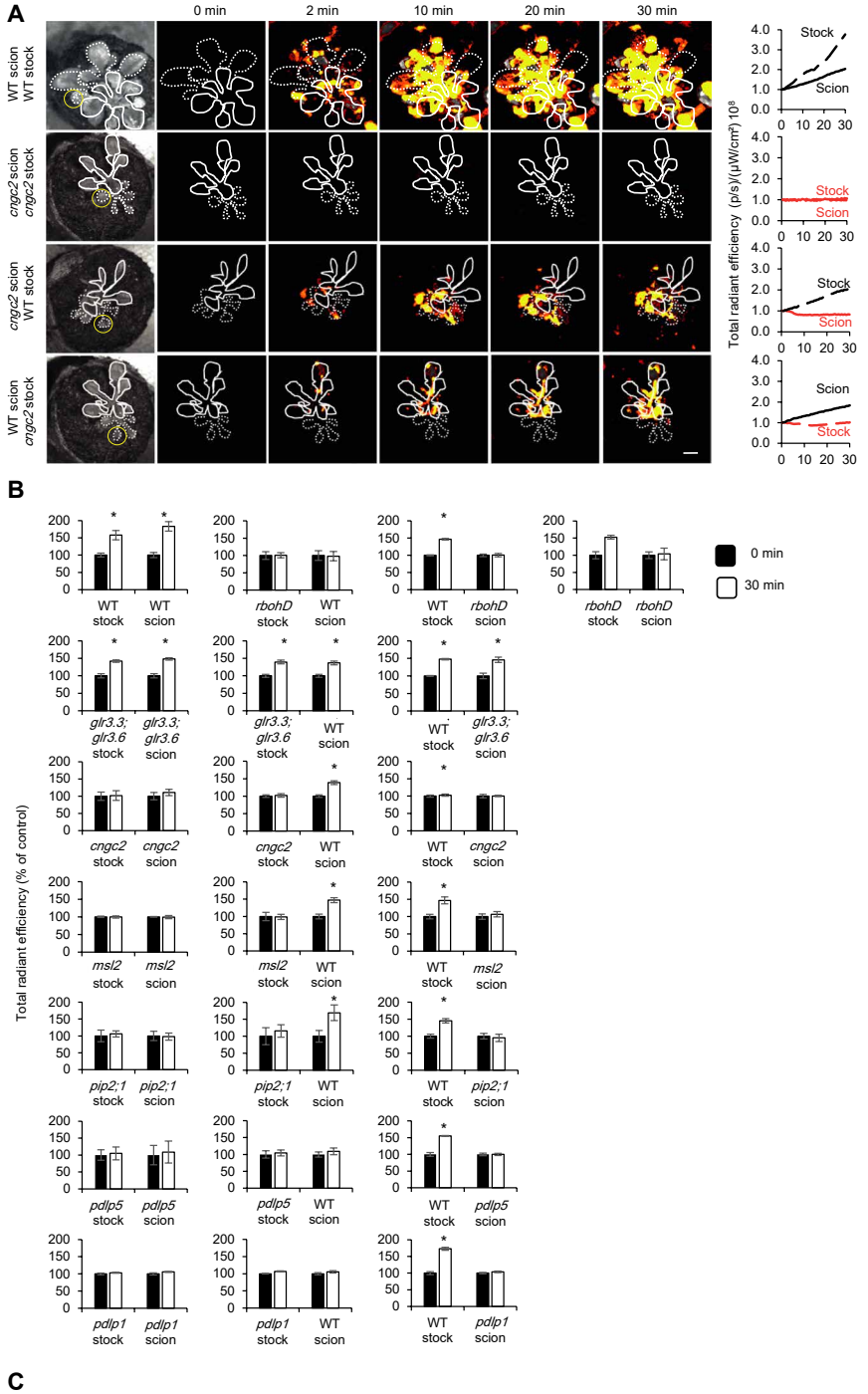

Fig. 4. The PD proteins PDLP1 and PDLP5, and RBOHD, are required for the initiation and propagation of the rapid systemic ROS signal. (**A**) Representative time-lapse images of systemic ROS accumulation and line graphs showing continuous measurements of ROS in the indicated grafting combinations between wild-type (black in line graphs) and the *cngc2* mutant (red in line graphs). Representative examples of line graphs for all other grafting combinations are shown in the Supplementary Materials (fig. S10). The areas of local stock leaves subjected to an HL stress treatment are indicated by yellow circles, scions are indicated by solid white lines, and stocks are indicated by dashed white lines. Scale bar, 1 cm. (**B**) Bar graphs showing the combined data from the stock and scion of the indicated grafting combinations using WT and *rbohD*, *glr3.3;glr3.6*, *cngc2*, *msl2*, *pip2;1*, *pdlp1*, and *pdlp5* mutants at the 0- and 30-min time points. (**C**) Graphical summary of the results obtained from experiments with the indicated grafting combinations. All experiments were repeated at least three times with 10 plants of each genotype per experiment. Data represent means ± SE. *$P < 0.05$, Student's *t* test.

Ca^{2+}-permeable channels GLR3.3 and GLR3.6 may only have a supportive role in mediating local HL stress–induced systemic ROS signals along the entire path (Figs. 1A, 3, A and B, and 4, B and C). It is further proposed that the function of two different pathways is required to mediate the rapid systemic ROS signal from its initiation site to the entire plant and induce SAA to a local HL stress treatment: (i) a cell-autonomous pathway that amplifies the systemic ROS signal, triggers acclimation responses, and requires RBOHD, GLR3.3, GLR3.6, PIP2;1, CNGC2, and MSL2 and (ii) a cell-to-cell pathway that propagates the systemic signal and requires RBOHD, PDLP5, and PDLP1 (Fig. 6). Because mutants impaired in *GLR3.3;GLR3.6*, *CNGC2*, *MSL2*, or *PIP2;1* were able to sense the HL stress at their local tissues but failed to enhance the expression of different acclimation transcripts at their systemic leaves, as well as failed to induce acclimation in their local or systemic leaves (Fig. 3, A and B), and because stocks made from these mutants were able to transfer the systemic signal to a wild-type scion but did not accumulate high ROS amounts themselves (Fig. 4, A to C, and fig. S10), it is possible that the role of the cell-autonomous pathway is to enhance the ROS signal, activate the expression of acclimation transcripts, and induce acclimation, in each cell along the path of the HL-induced systemic signal (Fig. 6). In contrast, PDLP5, PDLP1, and RBOHD, which were essential for transferring the systemic signal from the stock to the scion, local and systemic accumulation of ROS, the enhanced expression of acclimation transcripts in systemic tissues, and local and systemic acclimation (Figs. 2, A and B, 3, A and B, 4, B and C, and 5, A and B, and fig. S10), were required for both cell-to-cell systemic signal propagation and activation of acclimation responses during the systemic response of

Downloaded from http://stke.sciencemag.org/ on June 24, 2021

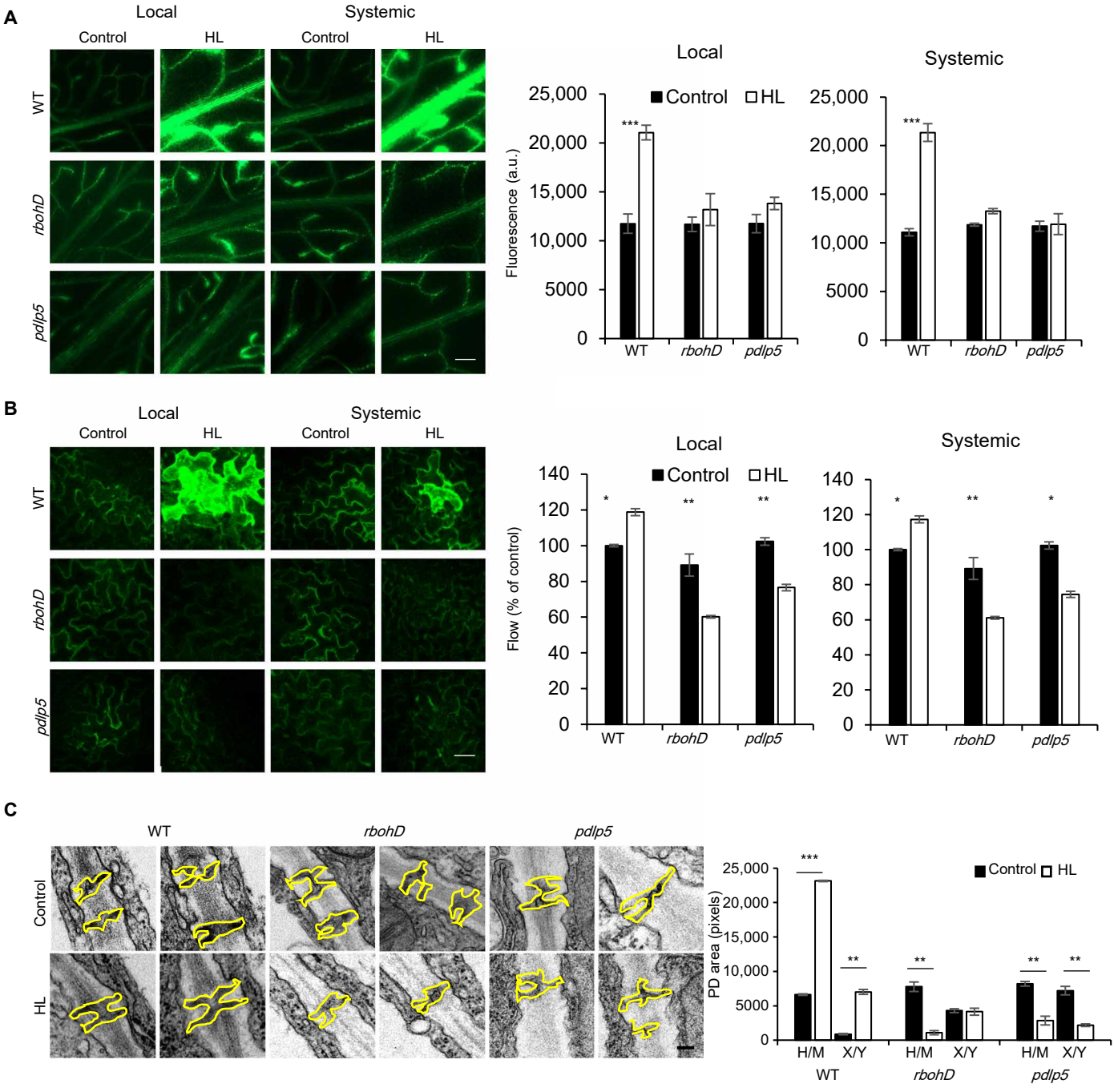

Fig. 5. *RBOHD* and *PDLP5* promote cell-to-cell spread of carboxyfluorescein and increase PD pore size during light stress responses in *Arabidopsis*. (**A**) Representative images and quantification of fluorescence intensity in vascular bundles of local and systemic carboxyfluorescein-loaded petioles of WT, *rbohD*, and *pdlp5* plants subjected to a local HL stress treatment (fig. S11A). Scale bar, 250 μm. Experiments were repeated 6 to 10 times per genotype with 10 biological repeats. $N = 60$ to 90 per genotype. Data represent means ± SE. $^{***}P < 0.005$, Student's *t* test. (**B**) Representative images and quantification of carboxyfluorescein fluorescence flow between different cell layers in local and systemic leaf cells of WT, *rbohD*, and *pdlp5* plants subjected to a local HL stress treatment (fig. S11A). Scale bar, 100 μm. Experiments were repeated six times with 10 biological repeats per genotype. Data represent means ± SE. $N = 60$ per genotype. Data represent means ± SE. $^{**}P < 0.01$ and $^{*}P < 0.05$, Student's *t* test. (**C**) TEM analysis of PD pore area in the petioles of local leaves of WT, *rbohD*, and *pdlp5* plants subjected to a local HL stress treatment (applied to the leaf area only; fig. S11B). Representative images of PD and quantification of PD pore area (H/M- and X/Y-shaped PDs) are shown. Scale bar, 0.1 μm. Experiments were repeated 6 to 10 times with 10 plants of each genotype per experiment. $N = 60$ to 100 per genotype. Data represent means ± SE. $^{***}P < 0.005$ and $^{**}P < 0.01$, Student's *t* test.

Downloaded from http://stke.sciencemag.org/ on June 24, 2021

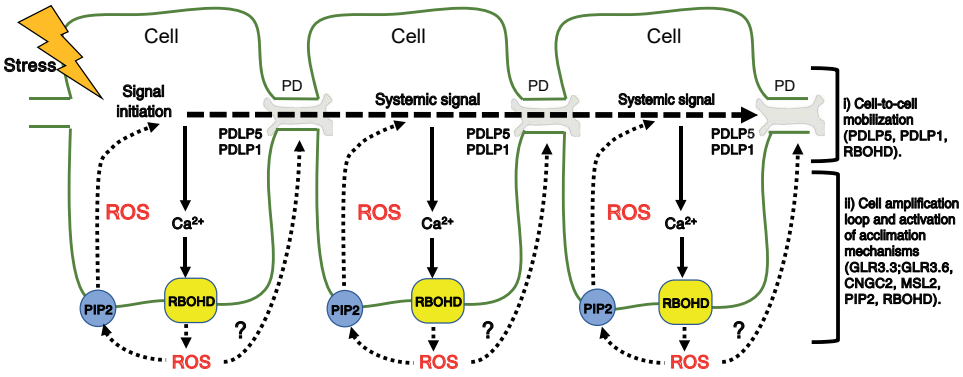

Fig. 6. A hypothetical model for ROS and PD interactions during systemic signaling in *Arabidopsis*. A hypothetical model for the regulation of rapid systemic ROS signaling by the different Ca^{2+}-permeable channels, ROS produced by RBOHD, PD, and aquaporin functions. Two pathways are proposed to regulate rapid systemic ROS signaling in plants: (i) a cell-to-cell pathway that involves PDLP5, PDLP1, and RBOHD and (ii) a cell-autonomous pathway (cell amplification loop) that amplifies and regulates the ROS and Ca^{2+} signals in each cell and involves RBOHD, GLR3.3;GLR3.6, CNGC2, MSL2, and PIP2. ROS produced by each cell along the path of the signal are depicted as regulating PD function. More detailed discussion is provided in the text. CNGC, cyclic nucleotide–gated ion channel; GLR, glutamate receptor–like; MSL, mechanosensitive channel of small conductance–like; PD, plasmodesmata; PDLP, PD-localized protein; PIP, plasma membrane intrinsic protein; RBOHD, respiratory burst oxidase homolog D; ROS, reactive oxygen species.

Arabidopsis to a local treatment of HL stress (Fig. 6). Because RBOHD function (ROS production) was required for both pathways (Figs. 4, B and C, 5, A to C, and 6), it is likely that ROS propagate from cell to cell or that ROS produced in each cell along the path of the systemic signal are required for propagating the systemic signal from cell to cell (Fig. 6). These functions could be mediated by low levels of ROS that are below the detection limit of the whole-plant ROS imaging method we used. In contrast, the activation of acclimation responses within each cell along the path of the signal (cell-autonomous pathway) could require high levels of ROS that are readily detected by the ROS imaging method we used (Fig. 4, A to C).

How could ROS be mobilized between cells or affect the transport of the rapid systemic signal? RBOHD-produced ROS could accumulate at the apoplast and enter the cells that produced them, or neighboring cells, through the aquaporin PIP2;1, and/or they could be mobilized between cells through PD after entering the cytoplasm through PIP2;1. Because PIP2;1 was not required for mobilizing the rapid systemic ROS signal through the stock to the scion in our grafting experiments, but PDLP5 and PDLP1 were (Fig. 4, B and C, and fig. S10), it is likely that ROS that enter cells through PIP2;1 are mobilized between cells through PD (Fig. 6). Alternatively, ROS could affect PD function from their cytosolic or apoplastic side (*45*) and/or affect the oxidation state and function of PDLPs (*39*, *42*–*44*), thus enabling rapid transport of the systemic signal (Fig. 6). ROS could, of course, use another, yet unidentified, route to enter neighboring cells. The proposed role for ROS in enhancing PD and tunneling nanotube transport in plant and mammalian cells (*45*), based in part on earlier studies in plants (*42*–*44*), could provide a key explanation to the role for ROS in cell-to-cell communication. The RBOHD-mediated production of ROS along the path of the systemic signal could play an important role in opening PD and promoting the transport of the systemic signal from cell to cell (Fig. 5, A and B).

PDLPs are required for pathogen-induced PD closure responses that involve callose deposition (*37*–*39*, *42*–*44*), in apparent conflict with the results presented here (Figs. 2, A and B, 3, A and B, 4, B and C, and 5, A and B). Because pathogen-induced PD closure responses, as well as callose deposition, could take hours to days after pathogen exposure to develop (*37*–*39*, *42*–*44*), whereas the responses to HL stress reported here occur within minutes (Figs. 1, A to C, 2, A to D, 3, A and B, 4, A to C, and 5, A and B), it is possible that PDLPs have multiple functions that may occur at different time scales or rates. They are involved in PD opening in response to a local HL stress–induced short burst of ROS (Fig. 5, A and B) but may induce PD closure over the long term in response to prolonged ROS accumulation and/or other pathogen-derived signals (*37*–*39*, *42*–*44*).

The finding that deletion of any one of several other Ca^{2+}-permeable channels and PD and aquaporin proteins (*MSL10*, *ANN1*, *OSCA1*, *TPC1*, *KIN7*, and *PIP1;2*) results in enhanced propagation rates of systemic ROS signals hints to the existence of additional, yet unknown, pathways that suppress systemic signals and/or alter their signatures. The remarkable differences observed between the spread of systemic ROS signals in the *pip1;2* and *pip2;1* mutants (Fig. 2, C and D), for example, could result from differential interaction of these two channels with other proteins in the cell, as well as their differential regulation by phosphorylation and/or acetylation (*32*, *50*), the differential stability of these two water channels in the presence of ROS (*51*), and/or the differential permeability of these two channels for H_2O_2 (*52*). In addition, because PIP2;1 primarily localizes to the vascular tissues in *Arabidopsis* (*31*, *32*), it could be directly required for mediating the propagation of the ROS wave through these same tissues (*22*). Systemic ROS signals could therefore be controlled by multiple different pathways, some promoting them and some suppressing or altering their signature (*3*, *4*, *8*, *24*). Supporting the existence of ROS wave–suppressing pathways is a study showing that the transcription factor MYB30 suppresses systemic ROS signals in response to a local application of HL stress (*21*).

Although the Ca^{2+}-permeable channels GLR3.3 and GLR3.6 are important for mediating SWRs (*7*, *10*, *13*, *23*), our findings reveal that these channels may only have a supportive role in mediating systemic ROS signals in response to a local application of HL stress (Figs. 1A, 3, A and B, and 4, B and C). This discrepancy raises the possibility that different systemic signal transduction pathways are triggered by different stimuli. Whereas some systemic signaling pathways, triggered, for example, by wounding, absolutely depend on GLR3.3 and GLR3.6 (*7*, *10*, *13*, *23*), others, such as those triggered by a local application of HL stress, do not (Figs. 1A, 3, A and B, and 4, B and C). At least in our hands, both wounding- and HL-triggered systemic signal transduction pathways require ROS production by RBOHD (*8*). An alternative explanation is, of course, that during responses to a local application of HL stress the roles of GLR3.3 and GLR3.6 are replaced by other Ca^{2+}-permeable channels such as CNGC2 or MSL2 (Figs. 1, B and C, 3, A and B, and 4, A to C).

Together, the findings presented here highlight a key role for PD and RBOHD-produced ROS in mediating systemic ROS signals and SAA to HL stress. In addition, they suggest that

Downloaded from http://stke.sciencemag.org/ on June 24, 2021

RBOHD-generated ROS could enhance cell-to-cell transport and PD pore size in a process that depends on the function of PDLPs. Such a mechanism could control the mobilization of many different systemic signals in plants, triggered by different abiotic, biotic, or developmental cues.

MATERIALS AND METHODS

Plant material, growth conditions, and stress treatments

Homozygous *A. thaliana* knockout lines (table S1) and wild-type plants were germinated and grown on peat pellets (Jiffy 7; Jiffy International) under controlled conditions of 10-hour/14-hour light/dark regime, 50 µmol photons s^{-1} m^{-2}, and 21°C for 4 weeks. Plants were subjected to a local HL stress treatment by illuminating a single leaf with 1700 µmol photons s^{-1} m^{-2} using a ColdVision fiber optic LED light source (Schott), as described earlier (*8*, *9*, *18*, *22*).

Grafting

Adding a scion to a seedling stock was performed according to published literature (*47*). Briefly, seeds were germinated on 0.5× Murashige and Skoog (MS) media plates. An incision was made in 7-day-old stock seedlings to insert a rosette scion into the cut while keeping the rosette of the stock plant intact. MS plates were incubated for 5 days in a growth chamber at 20°C under constant light (50 µmol photons s^{-1} m^{-2}; 20°C). Surviving grafted plants were transplanted to peat pellets and grown as described above for five more days before stress treatments. For each knockout line, four combinations were constructed and tested: wild type as the scion and the stock, the mutant line as the scion and the stock, mutant scion on wild-type stock, and wild-type scion on a mutant stock. Grafting was repeated 40 times for each combination of each line with about 40% yield.

ROS imaging

Plants were fumigated for 30 min with 50 µM 2′,7′-dichlorofluorescein diacetate (H_2DCFDA; Millipore-Sigma) in a glass container using a nebulizer (Punasi Direct) as previously reported (*8*, *20*–*22*). After fumigation, a local HL stress treatment was applied to a single leaf for 2 min. Images of dichlorofluorescein fluorescence were acquired using an IVIS Lumina 5 apparatus (Perkin Elmer) for 30 min. ROS accumulation was analyzed using Living Image 4.7.2 software (Perkin Elmer) using the math tools. Time-course images were generated, and radiant efficiency of regions of interest (ROIs) was calculated. Radiant efficiency is defined as fluorescence emission radiance per incident excitation and is expressed as (photons/s)/(µW/cm^2) (*8*, *20*–*22*). In each experiment, wild type was compared as control to one set of mutants representing a gene of interest. Because the initial intensity of the ROS signal was sometimes different between different experiments, depending on the physiological state of plants, time of day, and the phenotype of the mutants, the visualization range scale was set for each experiment separately (*8*, *20*–*22*). Visualization range scale was first set automatically by the computer based on the peak intensity of the entire experiment and then corrected manually so that the progression rate will be visualized and not saturated (*8*, *20*–*22*). This resulted in line graphs that were sometimes different in their initial start point between different experiments. All readings were therefore standardized to the same start point in all line graphs, and all bar graphs are expressed as percentage of control (wild type at 0 min). Each dataset includes SE of 8 to 12 technical repeats and a Student's *t* test score (*8*, *20*–*22*). Dye penetration controls (fig. S12) were performed by fumigation of plants with 0.3% (v/v) hydrogen peroxide (Fisher Scientific) for 10 min after the H_2DCFDA fumigation and acquisition of images in the IVIS Lumina S5 (*8*, *20*–*22*).

SAA assays

Leaf injury after light stress was measured using the electrolyte leakage assay, as described previously (*9*, *14*, *18*, *20*–*22*). Briefly, systemic acclimation to HL stress was tested by exposing a local leaf to HL stress (1700 µmol photons s^{-1} m^{-2}) for 10 min, incubating the plant under controlled conditions for 50 min, and then exposing the same leaf (local) or another younger leaf (systemic) to HL stress (1700 µmol photons s^{-1} m^{-2}) for 45 min. Electrolyte leakage was measured by immersing the sampled leaf in distilled water for 1 hour and measuring water conductivity with an Oakton CON 700 conductivity meter (Thermo Fisher Scientific). Samples were then boiled, cooled down to room temperature, and measured again for conductivity (total leakage). The electrolyte leakage was calculated as percentage of the conductivity before heating the samples over that of the boiled sample conductivity. Results are presented as percentage of control (electrolyte leakage from leaves not exposed to the light stress treatment). Experiments consisted of five repeats for each condition in each line. SE was calculated using Microsoft Excel; one-way analysis of variance (ANOVA) (confidence interval = 0.05) and Tukey post hoc test were performed with IBM SPSS 25.

Real-time quantitative polymerase chain reaction

To measure the transcriptional response of local and systemic leaves to a local HL stress treatment in 4-week-old plants, HL (1700 µmol photons s^{-1} m^{-2}) was applied to a single leaf for 2 or 10 min. Exposed leaf (local) and unexposed fully developed younger leaf (systemic) were collected for RNA extraction. RNA was extracted using a Plant RNeasy kit (Qiagen) according to the manufacturer's instructions. Quantified total RNA was used for complementary DNA synthesis (PrimeScript RT Reagent Kit, Takara Bio). Transcript expression was quantified by real-time quantitative polymerase chain reaction (qPCR) using iQ SYBR Green supermix (Bio-Rad Laboratories), as described in (*6*, *9*, *14*, *18*, *21*), with specific primers for the following: *ZAT12* (AT5G59820), 5′-TGGGAAGAGAGTGGCTTGTTT-3′ and 5′-TAAACTGTTCTTCCAAGCTCCA-3′; *ZAT10* (AT1G27730), 5′-ACTAGCCACGTTAGCAGTAGC-3′ and 5′-GTTGAAGTTTGACCGGAAGTC-3′; and *MYB30* (AT3G28910), 5′-CCACTTGGCGAAAAAGGCTC-3′ and 5′-ACCCGCTAGCTGAGGAAGTA-3′. Elongation factor 1α (5′-GAGCCCAAGTTTTTGAAGA-3′ and 5′-TAAACTGTTCTTCCAAGCTCCA-3′) was used for normalization of relative transcript levels. Results, expressed in relative quantity ($2^{-\Delta\Delta CT}$), were obtained by normalizing relative transcript expression (ΔC_T) and comparing it to control wild type from local leaf ($\Delta\Delta C_T$). The data represent 15 biological repeats and 3 technical repeats for each reaction. SE and Student's *t* test were calculated with Microsoft Excel.

Cell-to-cell spread of carboxyfluorescein

A PD permeability assay was carried out on the basis of (*48*), using two different experimental settings (fig. S11A). In the first experimental design, a single local leaf was subjected to a local HL stress treatment for 2 min, and plants were then incubated under normal conditions for 30 min to allow the systemic signal to spread. The local leaf and a systemic leaf from the same plant were then cut, and

Downloaded from http://stke.sciencemag.org/ on June 24, 2021

their petioles were dipped in 1 mM 5(6)-carboxyfluorescein diacetate (CFDA; excitation/emission 492/517 nm, Millipore-Sigma) for 5 min. CFDA is a membrane-permeable dye, which, upon cell entry, hydrolyzes to the fluorescent carboxyfluorescein compound. Leaves were then imaged using a Lionheart FX (BioTek) fluorescent microscope at ×10 magnification using the GFP filter settings. Fluorescence intensity was measured at the vascular bundles of leaves 5 mm from the detachment site using the Lionheart FX Gen5 image analysis mode (BioTek). Untreated plants were used as controls with six biological repeats. In the second experimental design (fig. S11A), after the local 2-min application of HL stress, a drop of 5 µl of CFDA was placed on the adaxial surfaces of the local and systemic leaves (*48*). After 30 min of incubation, Z-scan of the epidermis tissues was obtained with a confocal laser scanning microscope (Leica TCS SP8, Leica Microsystems), and the rate of flow was calculated on the basis of the increase in the number of fluorescent layers as the CFDA spread in the *z* axis between cells (*48*), comparing treated and untreated plants. Confocal images were acquired at the University of Missouri Molecular Cytology Core facility. No published work we are aware of suggests that any artifacts using this reporter would influence the work reported here.

Transmission electron microscopy

Local leaves of 4-week-old plants were subjected to a 2-min local HL stress treatment and processed for TEM as described in (*49*). Briefly, leaves were sampled and their petioles were sectioned and fixed in 2% paraformaldehyde and 2% glutaraldehyde in 100 mM sodium cacodylate buffer (pH 7.35) (fig. S11B). Samples were incubated at 4°C for 1 hour, rinsed with cacodylate buffer, and followed by distilled water. En bloc staining was performed using 1% aqueous uranyl acetate at 4°C overnight. Samples were then rinsed with distilled water. A graded dehydration series was performed using ethanol and transitioned into acetone, and dehydrated tissues were then infiltrated with a 1v/1v of Epon and Spurr resin for 24 hours at room temperature and polymerized at 60°C overnight. Sections were cut to a thickness of 80 nm using an ultramicrotome (Ultracut UCT, Leica Microsystems) and a diamond knife (Diatome). Images were acquired with a JEOL JEM 1400 transmission electron microscope (JEOL) at 80 kV on a Gatan Ultrascan 1000 charge-coupled device camera (Gatan, Inc.). The size of PDs in different vascular bundle and parenchyma cells was analyzed using ImageJ. Each experiment included 10 technical repeats and 20 biological repeats. Preparation of the samples and imaging were performed at the Electron Microscopy Core facility at the University of Missouri.

Statistical analysis

Statistical analysis for ROS accumulation (total radiant efficiency), real-time qPCR transcript expression, carboxyfluorescein fluorescence, and PD pore area size measurements was performed by two-sided Student's *t* test, and results are presented as means ± SE. $*P < 0.05$, $**P < 0.01$, and $***P < 0.001$. Statistical analysis for acclimation studies was performed by a one-way ANOVA followed by a Tukey post hoc test, and results are presented as means ± SE. Different letters denote statistical significance at $P < 0.05$.

SUPPLEMENTARY MATERIALS

stke.sciencemag.org/cgi/content/full/14/671/eabf0322/DC1

Fig. S1. Local and systemic ROS accumulation in the *glr3.3* or *glr3.6* mutants in response to a local application of HL stress.
Fig. S2. Local and systemic ROS accumulation in *msl3* mutants in response to a local application of HL stress.
Fig. S3. Local and systemic ROS accumulation in *msl10* mutants in response to a local application of HL stress.
Fig. S4. Local and systemic ROS accumulation in *ann1* mutants in response to a local application of HL stress.
Fig. S5. Local and systemic ROS accumulation in *osca1* mutants in response to a local application of HL stress.
Fig. S6. Local and systemic ROS accumulation in *tpc1* mutants in response to a local application of HL stress.
Fig. S7. Local and systemic ROS accumulation in *kin7* mutants in response to a local application of HL stress.
Fig. S8. Local and systemic ROS accumulation in *gat1* mutants in response to a local application of HL stress.
Fig. S9. Local and systemic ROS accumulation in *pip1;4* mutants in response to a local application of HL stress.
Fig. S10. ROS accumulation in local and systemic leaves of representative wild-type and mutant plants used to generate Fig. 4.
Fig. S11. The experimental setups used for the analyses shown in Fig. 5.
Fig. S12. Whole-plant ROS imaging after H_2O_2 fumigation into the different mutants.
Table S1. Detailed description of the different alleles used in this study.
Movie S1. ROS accumulation in wild-type and *glr3.3;glr3.6* plants subjected to a local treatment of HL stress.
Movie S2. ROS accumulation in wild-type and *cngc2* plants subjected to a local treatment of HL stress.
Movie S3. ROS accumulation in wild-type and *msl2* plants subjected to a local treatment of HL stress.
Movie S4. ROS accumulation in wild-type and *pdlp1* plants subjected to a local treatment of HL stress.
Movie S5. ROS accumulation in wild-type and *pdlp5* plants subjected to a local treatment of HL stress.
Movie S6. ROS accumulation in wild-type and *pip1;2* plants subjected to local treatment of HL stress.
Movie S7. ROS accumulation in wild-type and pip2;1 plants subjected to a local treatment of HL stress.

View/request a protocol for this paper from *Bio-protocol*.

REFERENCES AND NOTES

1. A. Y. Cheung, L.-J. Qu, E. Russinova, Y. Zhao, C. Zipfel, Update on receptors and signaling. *Plant Physiol.* **182**, 1527–1530 (2020).
2. J. K. Zhu, Abiotic stress signaling and responses in plants. *Cell* **167**, 313–324 (2016).
3. R. Mittler, ROS are good. *Trends Plant Sci.* **22**, 11–19 (2017).
4. H. Kollist, S. I. Zandalinas, S. Sengupta, M. Nuhkat, J. Kangasjärvi, R. Mittler, Rapid responses to abiotic stress: Priming the landscape for the signal transduction network. *Trends Plant Sci.* **24**, 25–37 (2019).
5. S. Karpinski, H. Reynolds, B. Karpinska, G. Wingsle, G. Creissen, P. Mullineaux, Systemic signaling and acclimation in response to excess excitation energy in Arabidopsis. *Science* **284**, 654–657 (1999).
6. G. Miller, K. Schlauch, R. Tam, D. Cortes, M. A. Torres, V. Shulaev, J. L. Dangl, R. Mittler, The plant NADPH oxidase RBOHD mediates rapid systemic signaling in response to diverse stimuli. *Sci. Signal.* **2**, ra45 (2009).
7. M. Toyota, D. Spencer, S. Sawai-Toyota, W. Jiaqi, T. Zhang, A. J. Koo, G. A. Howe, S. Gilroy, Glutamate triggers long-distance, calcium-based plant defense signaling. *Science* **361**, 1112–1115 (2018).
8. Y. Fichman, G. Miller, R. Mittler, Whole-plant live imaging of reactive oxygen species. *Mol. Plant* **12**, 1203–1210 (2019).
9. S. I. Zandalinas, S. Sengupta, D. Burks, R. K. Azad, R. Mittler, Identification and characterization of a core set of ROS wave-associated transcripts involved in the systemic acquired acclimation response of Arabidopsis to excess light. *Plant J.* **98**, 126–141 (2019).
10. Q. Q. Shao, Q. Gao, D. Lhamo, H. Zhang, S. Luan, Two glutamate- and pH-regulated Ca^{2+} channels are required for systemic wound signaling in *Arabidopsis*. *Sci. Signal.* **13**, eaba1453 (2020).
11. M. Szechyńska-Hebda, J. Kruk, M. Górecka, B. Karpińska, S. Karpiński, Evidence for light wavelength-specific photoelectrophysiological signaling and memory of excess light episodes in Arabidopsis. *Plant Cell* **22**, 2201–2218 (2010).
12. A. Christmann, E. Grill, J. Huang, Hydraulic signals in long-distance signaling. *Curr. Opin. Plant Biol.* **16**, 293–300 (2013).
13. S. A. R. Mousavi, A. Chauvin, F. Pascaud, S. Kellenberger, E. E. Farmer, GLUTAMATE RECEPTOR-LIKE genes mediate leaf-to-leaf wound signalling. *Nature* **500**, 422–426 (2013).

Downloaded from http://stke.sciencemag.org/ on June 24, 2021

14. N. Suzuki, G. Miller, C. Salazar, H. A. Mondal, E. Shulaev, D. F. Cortes, J. L. Shuman, X. Luo, J. Shah, K. Schlauch, V. Shulaev, R. Mittler, Temporal-spatial interaction between reactive oxygen species and abscisic acid regulates rapid systemic acclimation in plants. *Plant Cell* **25**, 3553–3569 (2013).
15. S. Gilroy, N. Suzuki, G. Miller, W. G. Choi, M. Toyota, A. R. Devireddy, R. Mittler, A tidal wave of signals: Calcium and ROS at the forefront of rapid systemic signaling. *Trends Plant Sci.* **19**, 623–630 (2014).
16. Z. Guo, F. Wang, X. Xiang, G. J. Ahammed, M. Wang, E. Onac, J. Zhou, X. Xia, K. Shi, X. Yin, K. Chen, J. Yu, C. H. Foyer, Y. Zhou, Systemic induction of photosynthesis via illumination of the shoot apex is mediated sequentially by phytochrome B, auxin and hydrogen peroxide in tomato. *Plant Physiol.* **172**, 1259–1272 (2016).
17. W. G. Choi, G. Miller, I. Wallace, J. Harper, R. Mittler, S. Gilroy, Orchestrating rapid long-distance signaling in plants with Ca^{2+}, ROS and electrical signals. *Plant J.* **90**, 698–707 (2017).
18. A. R. Devireddy, S. I. Zandalinas, A. Gómez-Cadenas, E. Blumwald, R. Mittler, Coordinating the overall stomatal response of plants: Rapid leaf-to-leaf communication during light stress. *Sci. Signal.* **11**, eaam9514 (2018).
19. F. K. Choudhury, A. R. Devireddy, R. K. Azad, V. Shulaev, R. Mittler, Local and systemic metabolic responses during light-induced rapid systemic signaling. *Plant Physiol.* **178**, 1461–1472 (2018).
20. S. I. Zandalinas, Y. Fichman, A. R. Devireddy, S. Sengupta, R. K. Azad, R. Mittler, Systemic signaling during abiotic stress combination in plants. *Proc. Natl. Acad. Sci. U.S.A.* **117**, 13810–13820 (2020).
21. Y. Fichman, S. I. Zandalinas, S. Sengupta, D. Burks, R. J. Myers Jr., R. Azad, R. Mittler, MYB30 orchestrates systemic reactive oxygen signaling and plant acclimation. *Plant Physiol.* **184**, 666–675 (2020).
22. S. I. Zandalinas, Y. Fichman, R. Mittler, Vascular bundles mediate systemic reactive oxygen signaling during light stress. *Plant Cell* **32**, 3425–3435 (2020).
23. E. E. Farmer, Y. Q. Gao, G. Lenzoni, J. L. Wolfender, Q. Wu, Wound- and mechanostimulated electrical signals control hormone responses. *New Phytol.* **227**, 1037–1050 (2020).
24. Y. Fichman, R. Mittler, Rapid systemic signaling during abiotic and biotic stresses: Is the ROS wave master of all trades? *Plant J.* **102**, 887–896 (2020).
25. U. Dubiella, H. Seybold, G. Durian, E. Komander, R. Lassig, C.-P. Witte, W. X. Schulze, T. Romeis, Calcium-dependent protein kinase/NADPH oxidase activation circuit is required for rapid defense signal propagation. *Proc. Natl. Acad. Sci. U.S.A.* **110**, 8744–8749 (2013).
26. M. E. Wilson, M. Mixdorf, R. H. Berg, E. S. Haswell, Plastid osmotic stress influences cell differentiation at the plant shoot apex. *Development* **143**, 3382–3393 (2016).
27. W. Tian, C. Hou, Z. Ren, C. Wang, F. Zhao, D. Dahlbeck, S. Hu, L. Zhang, Q. Niu, L. Li, B. J. Staskawicz, S. Luan, A calmodulin-gated calcium channel links pathogen patterns to plant immunity. *Nature* **572**, 131–135 (2019).
28. S. L. Richards, A. Laohavisit, J. C. Mortimer, L. Shabala, S. M. Swarbreck, S. Shabala, J. M. Davies, Annexin 1 regulates the H_2O_2-induced calcium signature in *Arabidopsis thaliana* roots. *Plant J.* **77**, 136–145 (2014).
29. F. Yuan, H. Yang, Y. Xue, D. Kong, R. Ye, C. Li, J. Zhang, L. Theprungsirikul, T. Shrift, B. Krichilsky, D. M. Johnson, G. B. Swift, Y. He, J. N. Siedow, Z. M. Pei, OSCA1 mediates osmotic-stress-evoked Ca^{2+} increases vital for osmosensing in *Arabidopsis*. *Nature* **514**, 367–371 (2014).
30. M. J. Evans, W. G. Choi, S. Gilroy, R. J. Morris, A ROS-assisted calcium wave dependent on the AtRBOHD NADPH oxidase and TPC1 cation channel propagates the systemic response to salt stress. *Plant Physiol.* **171**, 1771–1784 (2016).
31. O. Rodrigues, G. Reshetnyak, A. Grondin, Y. Saijo, N. Leonhardt, C. Maurel, L. Verdoucq, Aquaporins facilitate hydrogen peroxide entry into guard cells to mediate ABA- and pathogen-triggered stomatal closure. *Proc. Natl. Acad. Sci. U.S.A.* **114**, 9200–9205 (2017).
32. J. Qiu, S. A. McGaughey, M. Groszmann, S. D. Tyerman, C. S. Byrt, Phosphorylation influences water and ion channel function of AtPIP2;1. *Plant Cell Environ.* **43**, 2428–2442 (2020).
33. S. I. Zandalinas, R. Mittler, ROS-induced ROS release in plant and animal cells. *Free Radic. Biol. Med.* **122**, 21–27 (2018).
34. N. Smirnoff, D. Arnaud, Hydrogen peroxide metabolism and functions in plants. *New Phytol.* **221**, 1197–1214 (2019).
35. T. T. S. Lew, V. B. Koman, K. S. Silmore, J. S. Seo, P. Gordiichuk, S.-Y. Kwak, M. Park, M. C.-Y. Ang, D. T. Khong, M. A. Lee, M. B. Chan-Park, N.-H. Chua, M. S. Strano, Real-time detection of wound-induced H_2O_2 signalling waves in plants with optical nanosensors. *Nat. Plants* **6**, 404–415 (2020).
36. J. O. Brunkard, P. C. Zambryski, Plasmodesmata enable multicellularity: New insights into their evolution, biogenesis, and functions in development and immunity. *Curr. Opin. Plant Biol.* **35**, 76–83 (2017).
37. C. Cheval, S. Samwald, M. G. Johnston, J. de Keijzer, A. Breakspear, X. Liu, A. Bellandi, Y. Kadota, C. Zipfel, C. Faulkner, Chitin perception in plasmodesmata characterizes submembrane immune-signaling specificity in plants. *Proc. Natl. Acad. Sci. U.S.A.* **117**, 9621–9629 (2020).
38. J. D. Petit, Z. P. Li, W. J. Nicolas, M. S. Grison, E. M. Bayer, Dare to change, the dynamics behind plasmodesmata-mediated cell-to-cell communication. *Curr. Opin. Plant Biol.* **53**, 80–89 (2020).
39. J.-Y. Lee, X. Wang, W. Cui, R. Sager, S. Modla, K. Czymmek, B. Zybaliov, K. Van Wijk, C. Zhang, H. Lu, V. Lakshmanana, A plasmodesmata-localized protein mediates crosstalk between cell-to-cell communication and innate immunity in *Arabidopsis*. *Plant Cell* **23**, 3353–3373 (2011).
40. M. S. Grison, P. Kirk, M. L. Brault, X. N. Wu, W. X. Schulze, Y. Benitez-Alfonso, F. Immel, E. M. Bayer, Plasma membrane-associated receptor-like kinases relocalize to plasmodesmata in response to osmotic stress. *Plant Physiol.* **181**, 142–160 (2019).
41. Y. Benitez-Alfonso, M. Cilia, A. San Roman, C. Thomas, A. Maule, S. Hearn, D. Jackson, Control of *Arabidopsis* meristem development by thioredoxin-dependent regulation of intercellular transport. *Proc. Natl. Acad. Sci. U.S.A.* **106**, 3615–3620 (2009).
42. H. L. Rutschow, T. I. Baskin, E. M. Kramer, Regulation of solute flux through plasmodesmata in the root meristem. *Plant Physiol.* **155**, 1817–1826 (2011).
43. S. Stonebloom, J. O. Brunkard, A. C. Cheung, K. Jiang, L. Feldman, P. Zambryski, Redox states of plastids and mitochondria differentially regulate intercellular transport via plasmodesmata. *Plant Physiol.* **158**, 190–199 (2012).
44. G. H. Lim, M. B. Shine, L. De Lorenzo, K. Yu, W. Cui, D. Navarre, A. G. Hunt, J. Y. Lee, A. Kachroo, P. Kachroo, Plasmodesmata localizing proteins regulate transport and signaling during systemic acquired immunity in plants. *Cell Host Microbe* **19**, 541–549 (2016).
45. D. Liang, A salutary role of reactive oxygen species in intercellular tunnel-mediated communication. *Front. Cell Dev. Biol.* **6**, 2 (2018).
46. Y. Fichman, R. Mittler, Noninvasive live ROS imaging of whole plants grown in soil. *Trends Plant Sci.* **25**, 1052–1053 (2020).
47. K. Bainbridge, T. Bennett, P. Crisp, O. Leyser, C. Turnbull, Grafting in Arabidopsis, in *Arabidopsis Protocols*, J. J. Sanchez-Serrano, J. Salinas, Eds. (Humana Press, 2014), pp. 155–163.
48. W. Cui, X. Wang, J. Y. Lee, Drop-ANd-See: A simple, real-time, and noninvasive technique for assaying plasmodesmal permeability, in *Plasmodesmata. Methods in Molecular Biology (Methods and Protocols)*, M. Heinlein, Ed. (Humana Press, 2015), vol. 1217, pp. 149–156.
49. S. I. Zandalinas, L. Song, S. Sengupta, S. A. McInturf, D. A. G. Grant, H. B. Marjault, N. A. Castro-Guerrero, D. Burks, R. K. Azad, D. G. Mendoza-Cozatl, R. Nechushtai, R. Mittler, Expression of a dominant-negative AtNEET-H89C protein disrupts iron–sulfur metabolism and iron homeostasis in *Arabidopsis*. *Plant J.* **101**, 1152–1169 (2020).
50. J. Bellati, C. Champeyroux, S. Hem, V. Rofidal, G. Krouk, C. Maurel, V. Santoni, Novel aquaporin regulatory mechanisms revealed by interactomics. *Mol. Cell. Proteomics* **15**, 3473–3487 (2016).
51. M. M. Wudick, X. Li, V. Valentini, N. Geldner, J. Chory, J. Lin, C. Maurel, D. T. Luu, Subcellular redistribution of root aquaporins induced by hydrogen peroxide. *Mol. Plant* **8**, 1103–1114 (2015).
52. C. Hooijmaijers, J. Y. Rhee, K. J. Kwak, G. C. Chung, T. Horie, M. Katsuhara, H. Kang, Hydrogen peroxide permeability of plasma membrane aquaporins of *Arabidopsis* thaliana. *J. Plant Res.* **125**, 147–153 (2012).

Acknowledgments: We thank E. Farmer, C. Maurel, and G. Stacy for seeds. We thank the Arabidopsis Biological Resource Center for all additional seeds used in this study. **Funding:** This work was supported by funding from the NSF (IOS-1353886, MCB-1936590, IOS-1932639) and the University of Missouri. **Author contributions:** Y.F. and R.J.M. performed experiments and analyzed the data. D.G.G. conducted TEM analysis. R.M. and Y.F. designed experiments, analyzed the data, and wrote the manuscript. **Competing interests:** The authors declare that they have no competing interests. **Data and materials availability:** All data needed to evaluate the conclusions made in the paper are present in the paper or the Supplementary Materials.

Submitted 29 September 2020
Accepted 22 January 2021
Published 23 February 2021
10.1126/scisignal.abf0322

Citation: Y. Fichman, R. J. Myers Jr., D. G. Grant, R. Mittler, Plasmodesmata-localized proteins and ROS orchestrate light-induced rapid systemic signaling in *Arabidopsis*. *Sci. Signal.* **14**, eabf0322 (2021).

Downloaded from http://stke.sciencemag.org/ on June 24, 2021

Science Signaling

Plasmodesmata-localized proteins and ROS orchestrate light-induced rapid systemic signaling in *Arabidopsis*

Yosef Fichman, Ronald J. Myers Jr., DeAna G. Grant and Ron Mittler

Sci. Signal. **14** (671), eabf0322.
DOI: 10.1126/scisignal.abf0322

Orchestrating systemic ROS signaling in plants

Localized abiotic stresses induce systemic responses that protect plants from subsequent occurrences of the stress. Fichman *et al.* found that systemic acclimation to light stress in *Arabidopsis thaliana* required the enzyme RBOHD locally at sites of high light stress to generate reactive oxygen species (ROS) as well as throughout the plant to propagate a wave of systemic ROS signaling. Light stress–induced systemic ROS signaling depended on proteins localized to plasmodesmata, which are structures that connect the cytoplasm of adjacent plant cells, and was associated with increases in plasmodesmata pore size. Aquaporins and various Ca^{2+}-permeable ion channels facilitated systemic ROS signaling by amplifying the ROS signal in each cell along the path of the ROS wave. Together, these findings demonstrate the importance of cell-to-cell transport mechanisms for generating, amplifying, and propagating systemic ROS signaling in response to high light stress in *Arabidopsis*.

ARTICLE TOOLS http://stke.sciencemag.org/content/14/671/eabf0322

SUPPLEMENTARY MATERIALS http://stke.sciencemag.org/content/suppl/2021/02/19/14.671.eabf0322.DC1

RELATED CONTENT
http://stke.sciencemag.org/content/sigtrans/13/640/eaba1453.full
http://stke.sciencemag.org/content/sigtrans/13/640/eabb9505.full
http://stke.sciencemag.org/content/sigtrans/13/632/eaay3585.full
http://advances.sciencemag.org/content/advances/6/19/eaaz0478.full
file:/content

REFERENCES This article cites 50 articles, 24 of which you can access for free
http://stke.sciencemag.org/content/14/671/eabf0322#BIBL

PERMISSIONS http://www.sciencemag.org/help/reprints-and-permissions

Use of this article is subject to the Terms of Service

Science Signaling (ISSN 1937-9145) is published by the American Association for the Advancement of Science, 1200 New York Avenue NW, Washington, DC 20005. The title *Science Signaling* is a registered trademark of AAAS.

Copyright © 2021 The Authors, some rights reserved; exclusive licensee American Association for the Advancement of Science. No claim to original U.S. Government Works

Downloaded from http://stke.sciencemag.org/ on June 24, 2021